

# Optimal load management strategy for large electric vehicle charging stations with undersized charger clusters

Erdem Gümrükcü<sup>1</sup>  | Ferdinanda Ponci<sup>1</sup> | Antonello Monti<sup>1</sup> | Giuseppe Guidi<sup>2</sup> | Salvatore D'Arco<sup>2</sup> | Jon Are Suul<sup>2,3</sup>

<sup>1</sup>Institute for Automation of Complex Power Systems, E.ON Energy Research Center, RWTH Aachen University, Aachen, Germany

<sup>2</sup>SINTEF Energy Research, Trondheim, Norway

<sup>3</sup>Department of Energy Cybernetics, Norwegian University of Science and Technology, Trondheim, Norway

## Correspondence

Erdem Gümrükcü, Institute for Automation of Complex Power Systems, E.ON Energy Research Center, RWTH Aachen University, Mathieustrasse 10, 52074 Aachen, Germany  
Email: [erdem.guemruekcue@conerc.rwth-aachen](mailto:erdem.guemruekcue@conerc.rwth-aachen)

## Funding information

German Federal Ministry of Education and Research (BMBF), Grant/Award Number: 01DR18004; The Research Council of Norway; Open access funding enabled and organized by Projekt DEAL.

## Abstract

This study proposes a load management strategy for parking and charging facilities with the capacity to serve several hundreds of electric vehicles. The strategy is built upon two assumptions on power distribution systems of large charging stations: i) they are configured as clusters, each comprising a number of charging units for reduced cabling complexity, ii) the power delivery components (such as feeders and circuit breakers) of individual clusters are sized for load factors smaller than 100% to reduce the capital costs. Unless controlled, the load demand can concentrate into particular cluster(s) whereas other clusters can still tolerate additional demand. This may lead to avoidable load interruptions and, thus, reduced energy provision. To address this issue, a load management strategy that optimises the distribution of vehicles across the clusters and their charging profiles is proposed. The strategy is compared in simulation with a benchmark strategy in different commercial parking lot scenarios. The results demonstrate that the optimal management achieves identical demand fulfilment rates despite more pronounced load factor limitations as compared to the benchmark strategy. This can enable further reduction in system component sizing. In the tested scenarios, the proposed strategy leads to increased long term profits ranging between 12% and 43%.

## KEYWORDS

demand side management, electric vehicle charging, energy management systems, optimisation, scheduling

## 1 | INTRODUCTION

Electric vehicles (EV) are characterised by a shorter range and a significantly longer recharging period compared to fuel-based cars [1]. Due to the recent progress in battery technology, several EV models with sufficiently large drive range, which can cover most travel scenarios on a single charge, are now available in the market [2]. Nevertheless, unavailability of EV charging infrastructure remains a limiting factor for the fast adoption of EVs [3]. To remove the concerns of potential users, and to support electrification of road transport, the number of EV charging points must be increased. However, merely increasing the number of charging points may not solve all infrastructural requirements. The temporal characteristics of the charging demand can be challenging for

the power systems since simultaneous charging of many vehicles within a local area can lead to significant issues such as frequent voltage drops and accelerated ageing of transformers [4, 5]. Controlled charging is seen as the key to reduce the simultaneity of the charging load and, thus, as an enabler for efficient and sustainable e-mobility [6–8].

The majority of prior research on EV charging control focusses on the stations that have few charging units (CUs). However, the diffusion of EVs will increase the importance of centralised charging environments, that is, large charging stations (LCSs) with several hundreds of CUs. The literature studies in this field consider optimal scheduling [9, 10] and demand response schemes [11] to shape the load of LCSs. However, the issues related to electrical installation within parking have not been considered in these studies.

This is an open access article under the terms of the Creative Commons Attribution-NonCommercial-NoDerivs License, which permits use and distribution in any medium, provided the original work is properly cited, the use is non-commercial and no modifications or adaptations are made.

© 2021 The Authors. *IET Electrical Systems in Transportation* published by John Wiley & Sons Ltd on behalf of The Institution of Engineering and Technology.

## 1.1 | Contextualisation of the problem

There are not yet many existing charging stations comprising several hundred of CUs. Besides, comprehensive descriptions of LCS-suitable topologies can be found only in few sources in the literature such as Ref.[12, 13]. The most suitable topology for LCSs is still an open question that needs to be answered by further research. Nevertheless, this study highlights the importance of the internal structure of LCSs and argues that the selected configuration can introduce some important constraints that affect load management. To investigate this issue on a generic system topology that is practically applicable in several cases, this study assumes that the internal configurations of the future LCSs will fulfil two conditions. First, LCSs will be organised as charger clusters (CC) each consisting of a number of CUs due to space constraints. Second, as suggested by many studies that address optimal sizing of charging infrastructures, for example, Ref.[14, 15], power capability of the clusters will be smaller than the total installed power of the CUs for economic reasons. For simplicity, the systems where both conditions apply will be referred to as under-sized charger clusters (UCC) in this study.

A system configuration based on UCCs would be reasonable as a sound engineering practice for ensuring segmentation while limiting the cost of such large-scale installations. However, the heterogeneity of the parking profiles and energy demands of unscheduled parking and charging of EVs can cause the load demand to concentrate into particular clusters whereas other clusters can have remaining margins for increased loading. Such conditions may cause frequent reductions of the charging power due to the load factor limitations of UCCs, and consequently, lead to reduced energy provision to the EVs. To avoid such problems, the load must be controlled in a way that considers the constraints arising from the cluster-based configuration.

## 1.2 | Literature review

The literature on EV charge control addresses a variety of topics such as smart charging for cost minimisation [16], ancillary service provision [17], and admission control/queuing [18]. To solve these problems, a large number of distributed and centralised control schemes were proposed. The readers may refer to the review papers such as Ref.[19–21] for further theoretical analysis on alternative control schemes. In this section, we will mention few representative examples to give a general overview on state-of-the-art strategies and demonstrate the need for an original formulation to deal with the novel problem that is defined in Section 1.1.

In distributed charging control, several system components such as CUs and aggregators are equipped with some computing capability; therefore, the computational effort is shared among several entities. This also prevents the overall system operation in case of single point failures. Distributed control can be realised in decentralised and hierarchical schemes. In decentralised schemes, CUs compute and adjust

their schedules by communicating with the other EVs until a global equilibrium is achieved. Yin et al represents the load management problem of a charging station as a Stackelberg game in Ref.[22]; the EVs are selfish players, negotiating with each other and the aggregator to find an equilibrium to the power dispatch problem. Although it is advantageous to take decisions as a result of negotiations between players rather than a centralist approach that prioritises a single entity's objectives, the communication overhead to achieve the consensus makes the practicability questionable in scenarios with several hundreds of EVs.

Hierarchical schemes delegate control and computational load to multiple direct or indirect aggregators via a tree-like communication topology; they are, thus, neither fully centralised, nor fully decentralised [20]. In broader literature, hierarchical schemes are popular on multi-micro-grid (MMG) scheduling problems [23–25]. In the recent publications, bi-level approaches that decouple management of single micro-grid from MMG attracted significant interest. For example, Ref.[25] defines the power dispatching problem such that the upper level calculates a dynamic price that reacts to the changes in the operating conditions in a community integrated energy system and the lower level optimises the charging behaviour of EVs based on the dynamic price signal calculated by the upper level.

In contrast to distributed control, a single entity is responsible for decision making in a centralised control. Several authors proposed centralised strategies based on traditional optimisation techniques such as mixed integer linear programming [26] for LCSs. Optimisation-based centralised control techniques are robust and they guarantee optimality; on the other hand, they can be computationally expensive when dealing with large scale problems. To alleviate the computational effort and to increase scalability, some recent publications propose strategies based on machine learning. For a detailed review on machine learning approaches, the interested readers are advised to refer to Ref.[21, 27]. The ability to find a near optimal solution without the execution of an optimisation problem is the main advantage of learning-based strategies; therefore, they are applied mostly to deal with uncertainty in complex systems. On the other hand, unlike optimisation-based strategies, the optimality is not guaranteed in learning-based centralised schemes.

None of the load management/scheduling strategies introduced in prior publications takes into account the topology of the electrical installation in LCSs. A management strategy that considers also the operational constraints due to UCC-based topology is required. Although an UCC-based LCS appears similar to a multi-micro-grid system in terms of clustering, the methods proposed in available literature on MMG are likely to be sub-optimal for our problem. Here, special attention must be paid to the mobility of the loads. Since the individual micro-grids in an MMG system are usually owned by different entities or geographically separated, it is unlikely that a central entity is authorised to control the distribution of the incoming EVs into specific micro-grids; on the other hand, the operator of a clustered charging station can

allocate incoming EVs into clusters with an instruction command upon their arrivals. Therefore, it is recommendable to investigate a new strategy that considers the specific constraints and controllable features of cluster-based charging stations.

### 1.3 | Contributions of the paper

This work introduces a strategy that controls the charging schedules (optimal scheduling), the distribution of EVs into clusters (optimal allocation) and the short term power references of all CUs (optimal intervention). The proposed strategy optimises temporal and spatial distribution of the system load by considering the temporal variations of the electricity prices, the urgency of the charging demands and the load factor constraints of the under-sized clusters. Since it controls not only the charging but also the mobility of incoming EVs, the proposed strategy is, in essence, a parking management strategy. However, we will prefer the term load management as it mainly controls the electrical behaviour of the parking system. For the sake of simplicity, we will refer to the developed strategy as optimal strategy.

The key contributions of this study can be summarised as follows. First, this work highlights the impact of electrical installation within parking in the load management problem of LCSs and formalises this problem in a way that can be solved by optimisation algorithms. In this regard, rather than a specific topology, this work considers the common problems of cluster-based configurations in which each cluster has a smaller power capability than its installed power. Second, this study introduces an optimisation-based approach to systematically address the capacity constraints of cluster-based electrical installation.

This work demonstrates the effectiveness of the proposed optimal strategy by comparing its performance with a benchmark strategy that (1) does not optimise the charging schedules, (2) considers only the existing load distribution of the clusters when assigning an incoming EV to clusters, and (3) does not distinguish the urgencies of the charging demand when supply reduction is needed. The results show that the optimal strategy effectively increases the energy supply of the system in identically constrained scenarios. These results indicate that larger levels of under-sizing can be possible without decreasing the demand fulfilment performance thanks to optimal management. The high-level economic analysis conducted in this study shows that optimal management enables a remarkable increase in long-term profits.

## 2 | GENERAL PRINCIPLES FOR TOPOLOGY SELECTION

### 2.1 | Number and power level of charging units

The optimal number and power level of CUs in a LCS depends on the parking patterns. In case that the number of CUs are

less than the number of simultaneously present EVs, plugged EVs that occupy CUs without charging prevent other ones from getting connected. The extended stays after charging completion block the supply potential of the system. Increasing the number of CUs to avoid such blockages without increasing the power capability of the installation could pay off in the parking facilities where the cars are left for several hours such as the garages of residential and office buildings, airports and park-and-ride areas.

In case of long stays, slow charging is more favourable than fast charging. Typically, fast charging is requested only when the recharging demand is urgent, because of the high costs [28], and the accelerated battery ageing [29] in this mode. For this reason, LCS is a concept that is more applicable in the areas where slow charging modes are preferred.

### 2.2 | Cluster-based configuration

Installed power of an LCS with Level 2 AC chargers may reach several megawatts (MW). Elaborate discussions on suitable system topologies for MW level charging stations almost exclusively examined the systems with few high-power DC (fast) chargers [30, 31]. Despite the equivalent total power levels, there are clear distinctions between the stations with numerous low-power CUs and the ones with few high-power CUs. The most obvious difference is the importance of the space coverage of the equipment. The space constraints can be more pronounced in the parks accommodating hundreds of cars. In this case, it can be difficult to include additional electrical equipment and local balancing elements such as stationary battery storage systems and fuel cells as suggested for fast charging stations with few chargers [32].

Service reliability is an essential factor for topology selection of LCSs. In principle, it is desired to include dedicated feeders from the main bus to each CU as illustrated in Figure 1a. Such configuration enables to localise maintenance and faults, and, thus, to keep the majority of the system operable despite local interruptions. However, this approach may not be feasible in practice due to the space limitations and large number of CUs in LCSs.

Clustering ‘N’ number of CUs and connecting them into a cluster bus that is supplied by a dedicated cluster feeder decreases wiring complexity and space coverage over the fully paralleled systems. An overview of the generic cluster-based topology can be seen in Figure 1b.

### 2.3 | Sizing strategy

The conservative approach for sizing a charger cluster, that is, selecting physical components such as switch-gears and feeders requires consideration of the aggregated power of CUs to guarantee continuous operation under 100% loading. However, if full load is rarely expected, it may be desired to reduce the

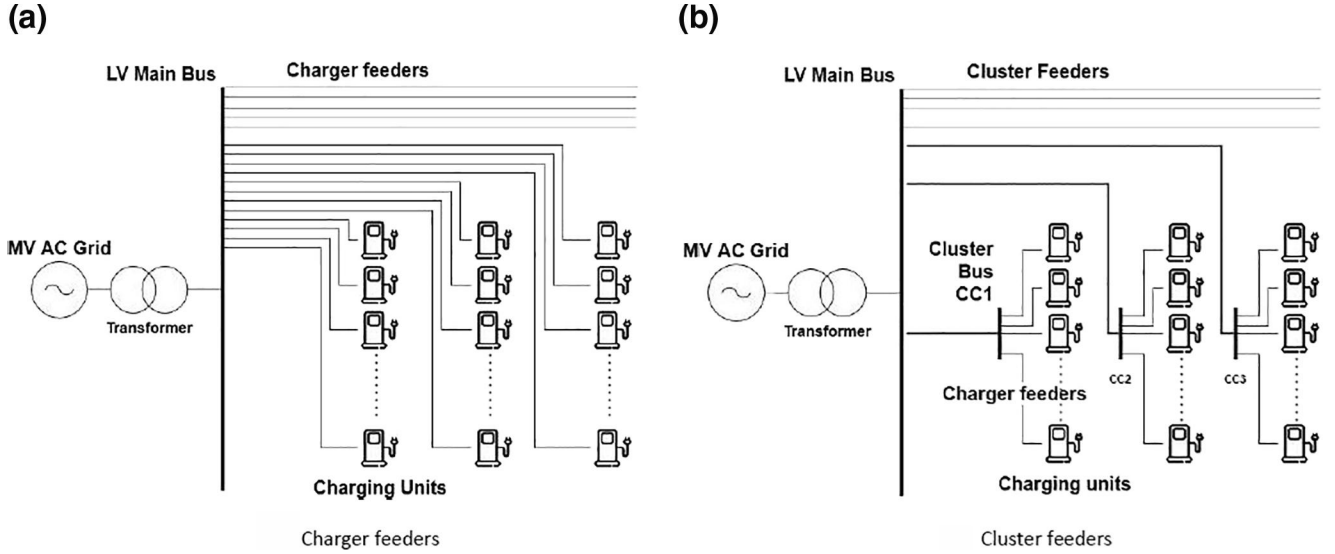


**FIGURE 1** Alternative layouts for large charging stations. (a) Each charging unit is connected to the main bus via a dedicated feeder. (b) Charging units are clustered and cluster buses are connected to the main bus via cluster feeders

capital costs with a proper under-sizing strategy. In this case, the physical components of a cluster are selected by considering a power level smaller than the total installed power of the chargers in the cluster,  $P_c$ .

It is important to notice that the considered under-sizing is not about the power ratings of the CUs. The CU rating is a design parameter whose effect is straightforward; the smaller sizing indicates the lower investment costs and also the lower supply capability in identical time periods. However, the relationship between sizing of the power delivery components of the clusters for example, cables and supply potential is rather complicated; it depends on how the charging profiles of multiple CUs are managed.

The quantification of sizing for physical components such as selection of cross-section of the cables and rating of the switch-gears is not within the scope of this study since they require careful examination of the physical constraints of the charging station such as dimensions and layout of the parking environment, length and thermal boundaries of the cables and number of cable joints. This study addresses sizing at higher level and uses total installed power of the clusters to define the ‘normal’ sizing of the system. Therefore, with  $P_c$  being the total installed power of the charging units in the cluster, the aggregated load of the cluster  $p_c(t)$  is hard-constrained by a reference value specified by the under-sizing parameter  $U$ :

$$p_c(t) \leq P_c \cdot (100\% - U\%) \quad (1)$$

The equivalent of the constraint (1) exists in broader charging control literature where capacity constraints of the entire charging station are considered such as Ref.[33]. This study applies such a constraint in each cluster of the LCS. This rule is enforced in the optimal intervention step of the proposed load management strategy.

### 3 | LOAD MANAGEMENT STRATEGY

The behaviour of a large-scale EV charging facility can affect the public electric grid in a complex way. However, in case of distribution grids with sufficient capacity, it can be assumed that the selected sizing, which determines the peak power of the station, guarantees that the activities in the charging station do not jeopardise the public grid operation. Therefore, the load management (LM) problem addressed in this study is considered to be independent from grid-side factors under normal operational conditions. This is also in line with the dominant tendency in the literature [34, 35] that decouples grid congestion and charging station management problems, and thus, defines different roles to the distribution system operator (DSO) and charging system operator (CSO).

The operational goals of a CSO are to fulfil the charging demands and minimise the charging costs under given constraints. The dynamics and constraints that need to be considered in LM can be summarised as follows. First, the energy stored in an EV battery increases with charging and is limited by the battery capacity  $E$ . Second, the number of cars connected in a CC increases with new EV allocations, and decreases with the departures of connected EVs. Third, the supply capability of a charging station is limited by the power rating  $P_{CU}$  of CUs, and can be limited due to under-sized CCs.

The LM strategy proposed in this work combines charging rate control and parking management in the charging station to deal with the constraints of UCC-based configuration. The strategy consists of three optimisation models that control the following:

1. the charging schedules of EVs (Scheduling);
2. the CUs where the incoming EVs should be connected (Allocation);
3. the short-term power references of all CUs (Intervention).

The energy demand and departure time of the hosted EVs should be known for calculating optimal scheduling, allocation and intervention decisions. This information indicates whether an EV can tolerate reduced charging rates and/or idle periods within the connection session. In this study, it is assumed that the energy capacity of the battery, state of charge (SOC), and the departure time are given by the users upon arrivals.

Based on the provided input, first, the scheduling model identifies the optimal (reference) charging schedule of the EV with the objective of charging cost minimisation. Second, the allocation model determines where to park (CU to connect) the EV. The optimal allocation aims to minimise unbalances between the load demands of clusters to avoid concentration of the demand in particular clusters. The intervention model runs periodically and updates the short term power references of all CUs by considering the individual schedules and capacity constraints of the UCCs. The three steps of the LM are illustrated in Figure 2.

### 3.1 | Optimal scheduling

This model calculates the reference schedule  $p^*$  of an incoming EV.  $p^*(t)$  specifies the power that is planned to be supplied along a particular time step  $[t, t + \Delta t) \subset [t_A, t_D)$  with  $t$ ,  $\Delta t$ ,  $t_A$  and  $t_D$  being, respectively, the time step identifier, length of one time step, arrival time and estimated departure time of the EV. This problem is formulated as a linear programme (LP). The LP defines the charging power constraint over a continuous range that is upper bounded by the rating of the charging unit  $P_{CU}$  as suggested by many authors in literature [24, 26, 36]:

$$0.0 \leq p^*(t) \leq P_{CU} \quad (2)$$

The scheduling problem is subject to constraints associated with the EV battery capacity  $E$ . These constraints are formalised via a dependent variable  $s^*(t)$ , representing the

reference SOC for  $t$ . Initial and final (target for departure) values of this variable,  $s^*(t_A)$  and  $s^*(t_D)$ , are given as optimisation parameters by the scenario. The SOC of the EV battery increases with charging according to the power conversion efficiency of the battery chargers,  $\eta$ . To model the dynamics of the SOC, the equations presented in Ref.[37] have been simplified and included in the optimisation model as optimisation constraints:

$$s^*(t + \Delta t) = s^*(t) + \frac{p^*(t) \cdot \eta \cdot \Delta t}{E} \quad (3)$$

$$s^*(t) \leq 100\% \quad (4)$$

The goal of schedule optimisation is minimisation of the charging cost. Therefore, the objective function weighs the power consumption price according to the temporal variations of the electricity price:

$$\min \sum_{t=A}^D W(t) \cdot p^*(t) \quad (5)$$

In broader literature, the time-of-use electricity price,  $\kappa^{el}(t)$ , is used as the equivalent of  $W(t)$  [36]. However, using constantly the same price signal to optimise the temporal behaviour of charge load is not efficient in LCSs; it can result in an aggregated load shape with excessively high peaks during low price windows. Such high peaks may require deviation from the optimal schedules due to the given power constraints (1) and, in certain scenarios, this may eventually reduce the energy supply of the LCS. This study suggests two rules to ensure optimum utilisation of supply potential while minimising the charging cost.

First, when the declared departure time,  $t_D$ , of an EV arriving in the charging station at  $t_A$ , denotes a parking duration that is shorter than a certain threshold, that is,  $t_D - t_A < T^{thr}$ , the cost-optimal scheduling is bypassed. In this

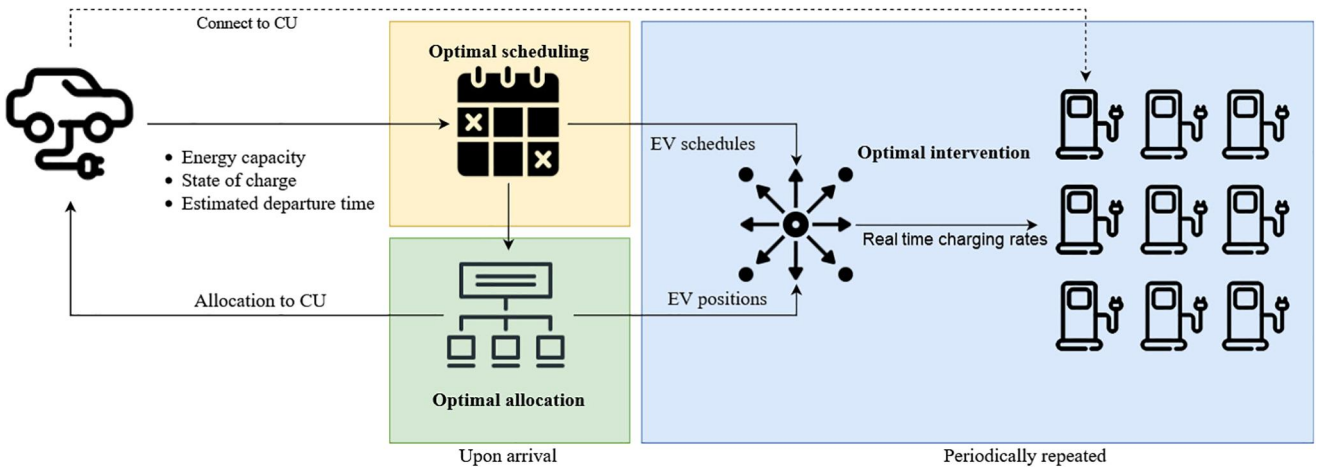


**FIGURE 2** Three steps of load management strategy: (i) Individual scheduling of the arriving EV, (ii) Allocation of the EV to one of the clusters considering the individual schedules, (iii) Updating the short-term power references of charging units

case, the schedule of the EV is equal to continuous charging with maximum power, that is,  $P_{CU}$  until the target SOC is reached:

$$p^*(t) = \begin{cases} P_{CU} & s^*(t) < s^*(t = t_D) \\ 0 & s^*(t) \geq s^*(t = t_D) \end{cases} \quad (6)$$

Second, the total required charging power,  $p_{\Sigma}^*(t)$ , calculated by summing up the schedules of all occupied CUs,  $p_{c,\mu}^*(t)$ , is compared with an effective upper limit for power consumption of the charging station,  $P^{max}(t)$ . The coefficients  $W(t)$  that penalise the power consumption at the time steps during which the scheduled system load exceeds this threshold are scaled up by the factor  $F$ :

$$W(t) = \begin{cases} \kappa^{el}(t) & p_{\Sigma}^*(t) < P^{max}(t) \\ (1 + F) \cdot \kappa^{el}(t) & p_{\Sigma}^*(t) \geq P^{max}(t) \end{cases} \quad (7)$$

In Ref.(7),  $P^{max}(t)$  is a dynamic parameter. Under normal operation, it is defined by the peak power capability of the charging station, that is, the under-sizing constraints of the clusters. However, in exceptional operational conditions, the DSO that is responsible for the public grid that the charging station is connected to can impose a time-varying power constraint,  $P_{dso}(t)$ . In practice, DSO constraint changes  $P^{max}(t)$  only when it is smaller than the peak power capability of the system:

$$P^{max}(t) = \begin{cases} P_{dso}(t) & P_{dso}(t) < P_{\Sigma} \cdot (1 - U\%) \\ P_{\Sigma} \cdot (1 - U\%) & P_{dso}(t) \geq P_{\Sigma} \cdot (1 - U\%) \end{cases} \quad (8)$$

### 3.2 | Optimal allocation

After solving the optimal scheduling problem, the optimal values of  $p^*(t)$  and  $s^*(t)$  are passed over to optimal allocation problem as optimisation parameters. Allocation is a combinatorial problem due to the finite number of options, that is, the CUs that an incoming EV can connect to. In our generic representation, the alternatives within a particular cluster are not distinguished. Therefore, the number of options are equal to number of the clusters. These options are formally represented by exclusive binary variables  $x_c$  with  $c$  representing a particular cluster among the set of clusters  $C$ . Equation (9) ensures that the EV is allocated to one and only one cluster.

$$\sum_c^C x_c = 1 \quad (9)$$

The first constraint that the optimal allocation problem is subject to is that the number of cars connected to the CUs of a cluster  $c$  cannot exceed  $N$  after the allocation of the new EV.

With  $I_c$  being the integer parameter that specifies the number of occupied CUs in the CC indexed by  $c$  before the allocation, this constraint is implemented as follows:

$$x_c + I_c \leq N \quad (10)$$

Considering the schedules of the connected EVs,  $p_{c,\mu}^*$ , and the schedule of the incoming EV,  $p^*$ , the scheduled load factor of the cluster  $c$  becomes  $I_c^*$  after allocation of the incoming EV. It is important to note that  $I_c^*$  is different from previous calculations only for the cluster  $c$  that the incoming EV is allocated to

$$I_c^*(t) = \frac{p^*(t) \cdot x_c + \sum_{\mu=1}^N p_{c,\mu}^*(t)}{P_{CU} \cdot N} \quad (11)$$

The objective function is selected based on the a priori knowledge that the higher inter-cluster loading unbalances denote the higher risk for local concentration of high load. A proactive control to avoid excessive loading in a particular cluster—while others' capacities are idle—increases the service capacity of the system. Therefore, the objective function of the allocation model presented by Ref.[38] which minimises the inter-phase and inter-arm unbalances of modular converter-based charging systems was adopted and modified for the general use:

$$\min \sum_{t=0}^T \sum_{c_1, c_2 \in \{C\}} |I_{c_1}^*(t) - I_{c_2}^*(t)| \quad (12)$$

where  $c_1$  and  $c_2$  indicate two clusters in the system. After solving the optimal allocation problem, the reference charge schedule and state of charge,  $p_{c,\mu}^*$  and  $s_{c,\mu}^*$ , of the identified CU are updated by the optimal scheduling results, that is,  $p^*$  and  $s^*$ , respectively. The new  $p_{c,\mu}^*$  and  $s_{c,\mu}^*$  values are taken as optimisation parameters in the following optimisation instances.

### 3.3 | Optimal intervention

The goal of the optimal intervention is to detect the situations that require deviation from  $p_{c,\mu}^*(t)$  within an optimisation horizon  $[t_0, t_F)$ , to find a new schedule  $p_{c,\mu}$  that minimises the deviation from reference SOC's at the end of the considered horizon  $s_{c,\mu}^*(t_F)$ , and to implement result at the current time step  $p_{c,\mu}(t_0)$  for a short period of time  $[t_0, t_0 + \Delta t)$ :

$$\min \sum_{c=1}^C \sum_{\mu=1}^N |s_{c,\mu}(t_F) - s_{c,\mu}^*(t_F)| \quad (13)$$

The objective function (13) penalises the deviations from the schedules calculated in the optimal scheduling step.

Therefore, the optimisation problem is a linear programme with the quadratic objective function. An important issue that needs to be considered in intervention decisions is that some of the EVs are expected to leave the charging station within the considered horizon  $[t_0, t_F)$  while others stay for longer periods. To link the EVs' presence into the intervention model, the expressions presented in Ref.[39] that specify the time period within which the EV can be charged is modified and included in the optimisation model:

$$0.0 \leq p_{c,u}(t) \leq \begin{cases} P_{CU} & t < t_{D,c,u} \\ 0 & t \geq t_{D,c,u} \end{cases} \quad (14)$$

where  $t_{D,c,u}$  represents the estimated departure time of the EV connected to  $c, u$ . While optimising  $p_{c,u}(t)$ , the power capability constraints of the charging station must be respected. At the highest-level of consideration, these constraints are the energy capacities of the EV batteries and power ratings of CUs and CCs. Therefore, the constraints (2)–(4) of the optimal scheduling model are transferred to the optimal intervention model by replacing  $p^*(t)$  and  $s^*(t)$  with  $p_{c,u}(t)$  and  $s_{c,u}(t)$ , respectively. Furthermore, the power capabilities of the under-sized clusters (1) are also considered as hard-constraints in the intervention model.

As stated earlier, the charging station is not in charge of managing the power flows in the public grid and the capacity that it can use is agreed upon before commissioning. However, when the operator of the public grid predicts or detects congestion due to external reasons, it can intervene in the operation of the charging station [40]. Without loss of generality, these interventions are included in the LM via the time-varying parameter that constrains the power consumption of the charging station,  $p_{dso}(t)$ , which is referred to as the DSO constraint:

$$\sum_c \sum_u^N p_{c,u}(t) \leq p_{dso}(t) \quad (15)$$

It is important to note that it is possible to modify the proposed LM to include application-specific restrictions other than equation (15) simply by adding new constraints to the optimal intervention model without modifying optimal scheduling and allocation models.

## 4 | PERFORMANCE METRICS

When the under-sizing constraints (1) dictate frequent reduction or suspension of power supply, some of the energy demand can remain unfulfilled. Therefore, as a cost reduction strategy, under-sizing has the potential drawback of decreasing the demand fulfilment. This part introduces the performance metrics to evaluate the proposed LM strategy in relation to the trade-off between demand fulfilment and investment cost.

### 4.1 | Demand fulfilment

The vehicle demand fulfilment rate  $f_v$  of the charging event  $v$  is the fraction of the charging demand that is met:

$$f_v = \frac{s_v(t_D) - s_v^*(t_A)}{s_v^*(t_D) - s_v^*(t_A)} \quad (16)$$

where  $s_v^*(t_A)$  is the arrival SOC of the EV that participated in the event  $v$ .  $s_v^*(t_D)$  and  $s_v(t_D)$  are, respectively, the targetted and achieved final SOC over the session.

A scenario indicated by  $V$  consists of  $|V|$  number of charging events that take place within the time window  $[t_{V0}, t_{VF})$ . To quantify the demand fulfilment performance at the system level, the scenario demand fulfilment rate,  $f_V$ , is used.  $f_V$  is the ratio of the charging events with certain individual fulfilment,  $X$ , to all charging events in  $V$ :

$$f_V(X) = \frac{|v \in V | f_v \geq X|}{|V|} \quad (17)$$

### 4.2 | Unit cost of charging

Unit cost of charging,  $q_V$ , is the average cost of provision of 1 MWh charging energy in scenario  $V$ . This term normalises the cost of daily electricity purchase with respect to the daily energy supply,  $e_V$ , and thus, allows to compare different scenarios and management strategies on a unified cost metric. With  $p_{\Sigma,V}(t)$  being the power that the charging station consumes at time step  $t$  in scenario  $V$  and  $\kappa^{el}(t)$  the time varying price of electricity,  $q_V$  is calculated as follows:

$$e_V = \sum_{t=t_{V0}}^{t=t_{VF}} p_{\Sigma,V}(t) \cdot \Delta t \quad (18)$$

$$q_V = \frac{\sum_{t=t_{V0}}^{t=t_{VF}} p_{\Sigma,V}(t) \cdot \Delta t \cdot \kappa^{el}(t)}{e_V} \quad (19)$$

### 4.3 | Long-term profit

Long-term economic impacts of different sizing and load management strategies are evaluated based on a high level cost–benefit analysis.

$$\pi = \rho - \kappa \quad (20)$$

$$\rho = \sum_{y=0}^{Y-1} \rho(y) \quad (21)$$

$$\kappa = \kappa^{ins} \cdot (1 + r)^Y + \sum_{y=0}^{Y-1} (\kappa^{gf}(y) + \kappa^{el}(y)) \quad (22)$$

$\pi$ ,  $\rho$  and  $\kappa$  are the net profit, total revenues and total costs of the charging station.  $\rho$  is the summation of the annual revenues within the period of  $Y$  years.  $\kappa$  is composed of the capital costs and operational costs. Capital cost is the installation cost of the charging station hardware,  $\kappa^{ins}$ , including EV chargers, transformers, distribution boards, cables, breakers etc.  $\kappa^{ins}$  is multiplied by the compound interest rate  $(1 + r)^Y$  to accurately estimate the value of the long-term investment. Operational cost is composed of two components. The first one,  $\kappa^{gf}(y)$  is the grid fee paid based on the capacity agreement between the charging station and the public grid operator in year  $y$ . The second one,  $\kappa^{el}(y)$  is the annual cost of electricity purchase. To estimate  $\kappa^{el}(y)$  and  $\rho(y)$ , it is assumed that the scenario  $V$  is repeated  $Z_y$  times over year  $y$  and the CSO gets a payment of  $\omega$  for each unit of energy that it provides to EVs.

## 5 | TEST SCENARIOS

### 5.1 | Parking lot

An example of commercial parking lot (CPL) was selected as the test environment. Behind this selection lies the expectation that, in high EV uptake scenarios, high occupancy rates during the day, that is, 7 AM–9 PM, will signal a noticeably high service potential, and thus, motivate the owners of such facilities to

equip their systems with large number of CUs. On the other hand, since the occupancy rates of CPLs decrease significantly at night, component under-sizing will be preferable for most CPLs. In this case, the LM strategy will play a key role to maximise the supply potential of the system within the peak hours where the load demand can exceed the given power capacity.

A charging infrastructure that consist of 6 equally sized clusters, as shown in Figure 3, was considered in the simulation scenarios. Each cluster has 50 charging units. The CUs are connected to the 3-phase cluster buses and have 11 kW power rating ( $P_{CU} = 11kW$ ). It was assumed that the power delivery components of the clusters are selected in such a way that the system operates stably as long as the constraint (1) is enforced. Therefore, the optimal intervention model introduced in Section 3.3 was used without any modification.

### 5.2 | Parking profiles and energy demand

To test the LM strategy, five scenarios with 400 parking events were generated. The number of events in the scenarios are equal to the number of EVs such that each EV visits the CPL once. Each of the five scenarios exhibits a unique distribution of long versus short-time parking events. The long-time events are performed by the full-time employees who work in the neighbourhood, arrive in their workplace between 8 and 9 AM in the morning and pick up their cars 7–10 h later. In the short-time events, the arrival times are randomly distributed over 7 AM–5 PM and the

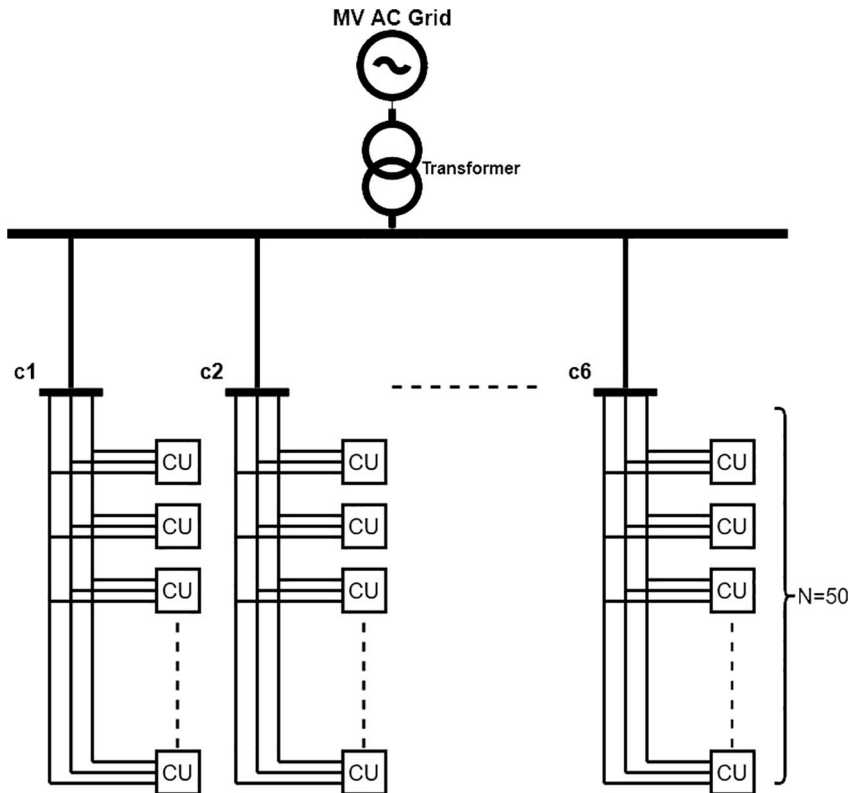


**FIGURE 3** Six equally sized clusters with  $50 \times 11kW$  CUs

parking duration between 1.5 and 3 h. The test scenarios are named after the percentage of the long-time events. For example, ‘Scenario30’ refers to the one where 30% of the parking events are performed by long-time visitors. The distribution of EV arrival/departures in the generated test scenarios are plotted in Figure 4.

In the test scenarios, each EV has 55 kWh battery capacity that can be charged with 11 kW 3-phase Type 2 chargers of the CPL. They arrive at the CPL with a randomly assigned SOC between 20% and 80%. Due to their randomly generated arrival/departure times, arrival SOC and charging demand, they can tolerate supply interruptions at various levels. To clarify the concept of tolerance, suppose an EV with a battery capacity of  $E$  arrives in the charging station with an SOC of  $s^*(t_A)$  at  $t_A$  and aims to leave with  $s^*(t_D)$  at  $t_D$ . With the given charger rating  $P_{CU}$ , it takes minimum  $T_M$  to supply the indicated energy demand. In this case, the EV can tolerate a supply interruption that lasts shorter than  $(t_D - t_A) - T_M$  of its parking duration. The tolerance,  $m$ , is defined to be relative to the total parking duration:

$$T_M = \frac{(s^*(t_D) - s^*(t_A)) \cdot E}{P_{CU}} \quad (23)$$

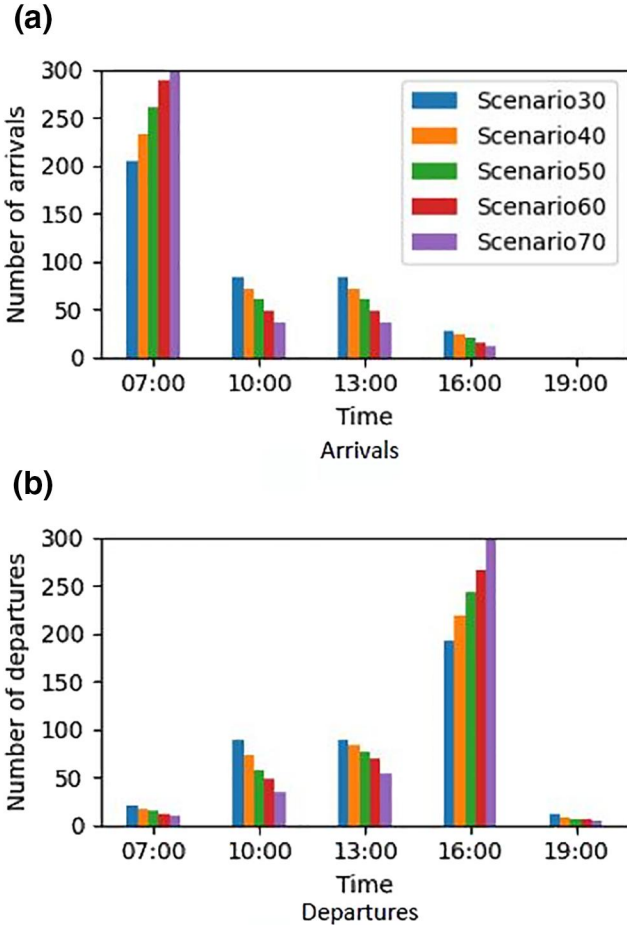


FIGURE 4 Distribution of arrival/departure times in test scenarios

$$m = \frac{t_D - t_A - T_M}{t_D - t_A} \quad (24)$$

The distribution of  $m$  in a scenario defines the difficulty for load management. If most/all of the EVs in a highly occupied cluster has low tolerance,  $m$ , the supply interruptions that are required due to the load factor limitations would also affect the demand fulfilment rates. Contrarily, larger  $m$  values facilitate dealing with the simultaneity of the charging demand as they allow temporal adjustments.

To quantify the tolerance level in the scenarios, and thus, inherent difficulty for LM, the events with very low (0%–20%), low (20%–40%), medium (40%–60%), high (60%–80%) and very-high (80%–100%)  $m$  values are grouped and their percentages among all events are presented in Table 1. In Scenario30, 51% of the EVs can tolerate interruptions that last shorter than 20% of their parking duration. In this scenario, only 4% of EVs can achieve the desired SOC when they do not receive any energy for more than 80% of their parking duration while the same tolerance category has 12% of the all EVs in Scenario70.

### 5.3 | Implementation of optimisation and simulation

The optimisation modelling package Pyomo [41] was used to deploy the LM algorithms in the simulations. The optimisation solver CPLEX [42] was used to solve the optimisation problems. The solver used the dual-simplex algorithm in the tests. Since the number of variables in the allocation problems is six in the tested case, the optimal allocation decisions were calculated through enumerations. The events were simulated in a Python programming environment with 5-min simulation resolution. Also, 5-min is the resolution with which the optimisation horizons are discretised in all three models, that is,  $\Delta t = 5 \times 60$  s.

Optimisation horizon of scheduling was adapted in each instance such that it equals to the parking duration of the incoming EV, that is,  $t_D - t_A$ . A constant optimisation horizon of 8 h was preferred in optimal allocations and interventions considering the regular parking duration in CPL. The European wholesale market prices that occurred on 6 January 2020 [43] were used to define the temporal variations in the electricity price  $\kappa^{el}(t)$ , which is plotted in Figure 5.

TABLE 1 Distribution of tolerance levels in test scenarios

| Tolerance | $m$      | Sce30 | Sce40 | Sce50 | Sce60 | Sce70 |
|-----------|----------|-------|-------|-------|-------|-------|
| Very low  | 0%–20%   | 51%   | 45%   | 38%   | 29%   | 21%   |
| Low       | 20%–40%  | 10%   | 7%    | 6%    | 5%    | 5%    |
| Medium    | 40%–60%  | 14%   | 16%   | 16%   | 19%   | 19%   |
| High      | 60%–80%  | 21%   | 22%   | 28%   | 35%   | 43%   |
| Very high | 80%–100% | 4%    | 10%   | 12%   | 12%   | 12%   |

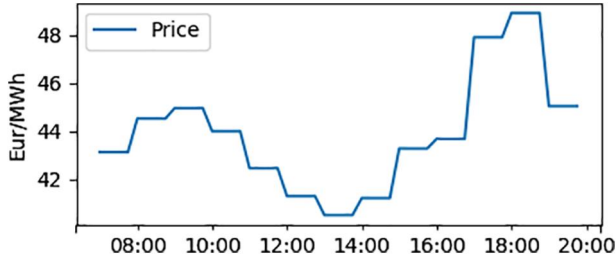


FIGURE 5 Temporal variations in electricity price

## 6 | INDIVIDUAL EVALUATION OF OPTIMAL SCHEDULING, ALLOCATION AND INTERVENTION MODELS

This section evaluates optimal scheduling, optimal allocation and optimal intervention models individually according to the sequence of their implementation. Each optimisation model is compared with a suitable benchmark strategy that controls the same variables as the corresponding step of the optimal LM strategy. The benchmark strategy for the scheduling step is equal to skipping schedule optimisation and selecting the schedules according to Ref.(6). In the allocation and intervention steps, the optimisation horizon of the benchmark strategies are limited with the current time step. This means that benchmark allocation sends an arriving car to the cluster that has the least load at the moment of arrival and benchmark intervention is agnostic to future departures.

Based on the comparisons, each sub-section recommends a particular strategy to control the relevant variables that is, schedules in Section 6.1, allocations in Section 6.2 and short-term power references in Section 6.3. Each subsection considers the recommendations provided in the precedent subsections. In this way, the final recommendation on the final sequenced approach of LM strategy is built step by step.

### 6.1 | Evaluation of scheduling strategy

This section evaluates the scheduling strategy according to the unit cost of charging,  $q_V$ . As mentioned earlier, in the benchmark strategy, the schedules are always determined by (6). Benchmark and optimal scheduling strategies were simulated in each scenario with varying under-sizing constraints  $U$ . Benchmark allocations and benchmark interventions were implemented in these simulations. In the optimal strategy, to specify the EVs with schedules to be optimised, the threshold  $T^{thr}$  was selected as 5 h. This selection enabled distinguishing long and short events; the schedules of the former were optimised with the cost-minimisation objective (5) while the latter were defined with the rule (6).

Table 2 shows the unit cost of charging,  $q_V$ , and total energy supply,  $e_V$ , in all simulated cases. The results highlight that optimal scheduling decreases  $q_V$  by 3%–7% in exact- ( $U = 0\%$ ) and low under-sizing scenarios ( $U = 25\%$ ). The impact of the selected scheduling strategy on  $q_V$  decreases

TABLE 2 Unit cost of charging (Eur/MWh) and total energy supply (kWh) with benchmark versus optimal scheduling

|       | Metric    | $U = 0\%$ |      | $U = 25\%$ |      | $U = 50\%$ |      |
|-------|-----------|-----------|------|------------|------|------------|------|
|       |           | Ben-      | Opt- | Ben-       | Opt- | Ben-       | Opt- |
| Sce30 | Supply    | 9247      | 9247 | 9247       | 9241 | 9199       | 9102 |
|       | Unit cost | 43.7      | 42.5 | 43.7       | 42.5 | 43.6       | 42.7 |
| Sce40 | Supply    | 9442      | 9442 | 9442       | 9432 | 9265       | 9274 |
|       | Unit cost | 43.8      | 42.3 | 43.8       | 42.4 | 43.7       | 42.6 |
| Sce50 | Supply    | 9687      | 9687 | 9673       | 9667 | 9428       | 9415 |
|       | Unit cost | 43.9      | 42.1 | 43.8       | 42.2 | 43.6       | 42.5 |
| Sce60 | Supply    | 9947      | 9947 | 9903       | 9889 | 9596       | 9464 |
|       | Unit cost | 43.9      | 41.8 | 43.9       | 42.0 | 43.4       | 42.4 |
| Sce70 | Supply    | 8479      | 8479 | 8447       | 8473 | 8362       | 8269 |
|       | Unit cost | 44.3      | 41.4 | 44.2       | 41.6 | 43.5       | 42.1 |

slightly when the under-sizing is higher ( $U = 50\%$ ). In Scenario30, Scenario60 and Scenario70, the cost reduction is accompanied by a 1% decrease in the  $e_V$ . However, this effect is scenario dependent; in Scenario40 and Scenario50, optimal scheduling saves 3% of charging cost without a noteworthy change in energy supply. Therefore, it is recommended to implement the optimal scheduling strategy to operate LCSs with UCCs.

### 6.2 | Evaluation of allocation strategy

This section investigates the impact of the allocation strategy on the total energy supply of the charging station,  $e_V$ . For this purpose, several simulations were performed by implementing both benchmark allocation and optimal allocation on the test scenarios. As recommended in Section 6.1, the optimal scheduling strategy was implemented in these simulations. Furthermore, to observe only the impact of allocations, an optimisation horizon of 5 min was considered in the intervention step (benchmark intervention) as done in Section 6.1.

Figure 6 depicts the aggregated power profile of the charging station in Scenario30 for  $U = 0\%$  and  $U = 50\%$ . In this scenario, system load exceeds 1650 kW, that is, 50% of the total installed capacity at 13:00 if the system is exact-sized. In case of 50% under-sizing, it is not possible to follow the reference schedules between 13:00 and 15:00; therefore, the load must be curtailed. Figure 6 shows that, for  $U = 50\%$ , optimal allocation enables energy supply at maximum power continuously between 13:00 and 15:00. At the same window, 527.6 kWh (15.4%) less energy is supplied through benchmark allocations. Although this difference is mostly compensated in the following hours, the cumulative energy supply in optimal allocation is 28 kWh (0.3%) larger as compared to benchmark. Likewise, some of the charging shifted to slightly more expensive period, the unit cost of charging increased by 0.1 Eur/MWh (0.4%).

The same procedure was applied in all scenarios for various under-sizing levels. Table 3 shows the cumulative energy supply in all simulated scenarios. For  $U = 50\%$ , optimal allocation performs slightly better than benchmark allocations in Scenario30 and Scenario50. At this under-sizing level, Scenario40 is the only exception where optimised allocations lead to small decrease in energy supply. On the other hand, in the scenarios with high percentage of long-time events, that is, Scenario60 and Scenario70, optimal allocations increase the energy supply by 2.5%. The simulation results of the heavily under-sized scenarios, that is, for  $U = 75\%$  demonstrate that the optimal allocations affect the energy supply significantly in the positive direction. In Scenario70, the increase enabled by the optimisation is 36%. Due to the increased supply in high under-sizing scenarios, it is recommended to implement optimal allocation in LCSs with UCCs.

### 6.3 | Evaluation of optimal intervention model

As expressed in Section 3.3, this model finds the optimal charging rates to implement at the current time step. The benchmark intervention model is agnostic to the future departures as its optimisation horizon spans only the current time

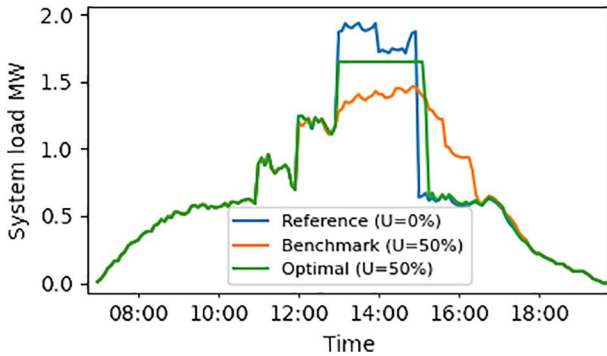


FIGURE 6 Aggregated power profiles in Scenario30 with benchmark versus optimal allocation

TABLE 3 Energy supply with benchmark vs optimal allocations

| $U$ | Strategy  | Sce30 | Sce40 | Sce50 | Sce60 | Sce70 |
|-----|-----------|-------|-------|-------|-------|-------|
| 0%  | Benchmark | 9247  | 9442  | 9687  | 9947  | 8479  |
|     | Optimal   | 9247  | 9442  | 9687  | 9947  | 8479  |
| 25% | Benchmark | 9241  | 9432  | 9667  | 9899  | 8473  |
|     | Optimal   | 9247  | 9442  | 9669  | 9887  | 8479  |
| 50% | Benchmark | 9102  | 9274  | 9415  | 9464  | 8269  |
|     | Optimal   | 9130  | 9229  | 9470  | 9703  | 8478  |
| 75% | Benchmark | 7284  | 7025  | 6736  | 6443  | 5571  |
|     | Optimal   | 7447  | 7331  | 7546  | 7660  | 7554  |

step. On the contrary, the optimal intervention takes into account the departures that will take place in the next 8 h. To evaluate the impact of forward-looking (optimal) intervention, all scenarios were simulated by implementing both benchmark and optimal interventions alongside with optimal scheduling and optimal allocations.

Table 4 compares the energy supply in different cases. In low under-sizing scenarios, the impact of forward-looking optimisation is limited. For  $U = 25\%$ , the resulting energy supply in benchmark and optimal interventions are almost same. The impact of extended optimisation horizon is more significant in highly under-sized scenarios. For  $U = 50\%$  in all scenarios except Scenario70, optimal intervention increases energy supply between 1% and 2.5%. For  $U = 75\%$ , the difference made by optimal intervention is 8% in Scenario30, 9% in Scenario40%, 6% in Scenario50, 5% in Scenario60%, and 4% in Scenario70.

Based on the demonstrated advantages of optimal intervention, that is, extended foresight, it is recommended to implement optimal interventions to control short time power references.

## 7 | OVERALL EVALUATION OF THE OPTIMAL LOAD MANAGEMENT

In Section 6, each of the three steps of the proposed (optimal) LM strategy is evaluated individually through comparison of benchmark versus optimal scheduling, benchmark versus optimal allocation and benchmark versus optimal intervention. Based on the comparisons, it is recommended to implement optimal scheduling, optimal allocation and optimal intervention rather than corresponding benchmarks. This section evaluates the three-step optimal LM strategy as a whole by comparing the resulting performance metrics against the results of the simulations where all steps are replaced with the corresponding benchmark strategy. For convenience, the combination of optimal scheduling, optimal allocation and optimal intervention will be referred to as optimal LM and the combination of benchmark scheduling, benchmark allocation and benchmark intervention as benchmark LM.

TABLE 4 Energy supply with benchmark vs optimal intervention

| $U$ | Strategy  | Sce30 | Sce40 | Sce50 | Sce60 | Sce70 |
|-----|-----------|-------|-------|-------|-------|-------|
| 0%  | Benchmark | 9247  | 9442  | 9687  | 9947  | 8479  |
|     | Optimal   | 9247  | 9442  | 9687  | 9947  | 8479  |
| 25% | Benchmark | 9247  | 9442  | 9669  | 9887  | 8447  |
|     | Optimal   | 9247  | 9442  | 9687  | 9947  | 8479  |
| 50% | Benchmark | 9130  | 9229  | 9470  | 9703  | 8478  |
|     | Optimal   | 9247  | 9442  | 9687  | 9947  | 8479  |
| 75% | Benchmark | 7447  | 7331  | 7546  | 7660  | 7554  |
|     | Optimal   | 8037  | 7979  | 8031  | 8018  | 7865  |

## 7.1 | Impact of DSO constraint

This sub-section investigates the response of the optimal LM to the DSO's interventions. In the investigated scenario, the DSO predicts a congestion in the grid for the following day. It informs the CSO about a curtailment, which constrains the power consumption of the charging station with 25% of its total installed capacity in the morning and evening hours; with 50% around noon, assuming that some of the congestion will be relieved thanks to PV generation.

$$P_{dso}(t) = \begin{cases} 25\% \cdot P_{\Sigma} & 06:00 \leq t < 10:00 \\ 50\% \cdot P_{\Sigma} & 10:00 \leq t < 16:00 \\ 25\% \cdot P_{\Sigma} & 16:00 \leq t < 20:00 \end{cases} \quad (25)$$

Five scenarios were simulated with consideration of  $P_{dso}$  for  $U = 50\%$  case. As the system load factor is already restricted by 50% due to under-sizing, the constraint imposed by the DSO does not require any further limitation in the power consumption within 10:00–16:00 interval. Figure 7 shows how the DSO constraint affects the power profile of the charging station under optimal LM in Scenario50.

Table 5 shows the energy supply for all simulated cases without and with consideration of the DSO constraint in the benchmark and optimal LM. The simulation results show that the DSO constraint leads to 4%–12% reduction in total energy supply of the system under benchmark LM. However, the optimal LM achieved the identical supply potential in spite of the DSO constraint.

## 7.2 | Benchmark and optimal sizing

This section investigates the maximum under-sizing level that can be achieved without appreciable decrease of the demand fulfilment rates. In the evaluations, the under-sizing levels that allow to meet the following condition are considered to be achievable:

$$f_V(99\%) = 100\% \quad (26)$$

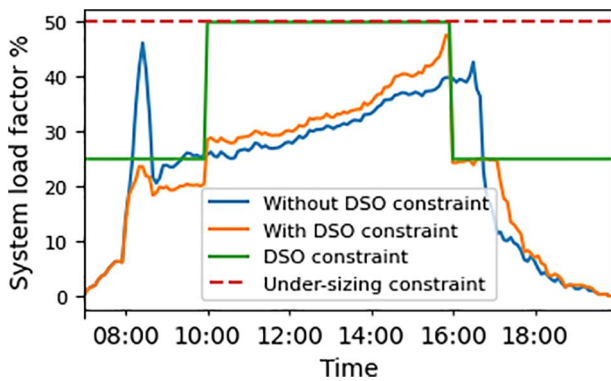


FIGURE 7 Aggregated power profiles in Scenario50 for  $U = 50\%$  without and with DSO constraint

Before benchmark versus optimal LM comparisons, the impact of small variations in scenarios on the results obtained via the benchmark LM was analysed. Therefore, the scenarios were modified by shortening/extending the duration of each parking event by a random factor, which is drawn randomly from the  $\pm 50\%$  range for the short and  $\pm 10\%$  for the long events. The percentage of the events where the condition (26) is met in each original and modified scenario can be seen in Table 6. These results indicate that the small variations in scenarios related to the duration of the parking events do not influence the demand fulfilment performance of benchmark LM significantly. Therefore, the maximum  $U$  values that meet the condition (26) in the original scenarios can be considered as maximum under-sizing levels that can be achieved by benchmark LM. These levels will be referred to as benchmark sizing in the analyses. The maximum  $U$  levels that fulfil the condition (26) via the optimal LM strategy were obtained with the same approach and are defined as optimal sizing.

Table 7 presents the maximum under-sizing that can be achieved via each LM strategy. In all tested scenarios, optimisation enables significantly larger under-sizing. The difference between benchmark versus optimal sizing increases with the increased percentage of long-time events in the scenario. In Scenario30, the system could be under-sized by 65% instead of

TABLE 5 Energy supply for benchmark and optimal LM under DSO constraint

| Scenarios | Benchmark LM           |                     | Optimal LM             |                     |
|-----------|------------------------|---------------------|------------------------|---------------------|
|           | Without DSO constraint | With DSO constraint | Without DSO constraint | With DSO constraint |
| Scce30    | 9199                   | 8783                | 9247                   | 9247                |
| Scce40    | 9265                   | 8832                | 9442                   | 9442                |
| Scce50    | 9428                   | 9029                | 9687                   | 9687                |
| Scce60    | 9596                   | 9262                | 9947                   | 9947                |
| Scce70    | 9362                   | 8277                | 8479                   | 8479                |

TABLE 6 Demand fulfilment ( $f_V(99\%)$ ) under original and modified scenarios

| Scenario |          | $U = 10\%$ | $U = 20\%$ | $U = 30\%$ | $U = 40\%$ | $U = 50\%$ |
|----------|----------|------------|------------|------------|------------|------------|
| Scce30   | Original | 100%       | 100%       | 100%       | 100%       | 89%        |
|          | Modified | 100%       | 100%       | 100%       | 100%       | 89%        |
| Scce40   | Original | 100%       | 100%       | 100%       | 90%        | 86%        |
|          | Modified | 100%       | 100%       | 100%       | 91%        | 86%        |
| Scce50   | Original | 100%       | 100%       | 94%        | 90%        | 86%        |
|          | Modified | 100%       | 100%       | 93%        | 92%        | 85%        |
| Scce60   | Original | 100%       | 95%        | 93%        | 88%        | 86%        |
|          | Modified | 100%       | 96%        | 93%        | 91%        | 86%        |
| Scce70   | Original | 96%        | 95%        | 95%        | 95%        | 94%        |
|          | Modified | 97%        | 97%        | 97%        | 96%        | 95%        |

**TABLE 7** Maximum reasonable under-sizing via benchmark vs optimal LM

| Management strategy | Sce30 | Sce40 | Sce50 | Sce60 | Sce70 |
|---------------------|-------|-------|-------|-------|-------|
| Benchmark LM        | 40%   | 30%   | 20%   | 10%   | 5%    |
| Optimal LM          | 65%   | 60%   | 60%   | 60%   | 70%   |

40% thanks to optimal LM. In Scenario50, where the percentage of long and short events are equal, the system could be under-sized by 60% instead of 20%. In Scenario70, 70% under-sizing is still possible by optimal LM whereas it should be no more than 5% if the load is controlled by the benchmark strategy.

The further under-sizing, enabled by optimal LM, reduces the impact of the charging station on the public grid. Even in the least affected scenario, Scenario30, the peak power that the charging station consumes decreases by 825 kW, which accounts for 25% of the total installed capacity of the station.

In a real system, the layout of the parking environment can be subject to various constraints, which necessitate different clustering approaches. It is important to note that the goal of this discussion is not to give recommendations on system design for a specific use case but demonstrating that the optimal LM is an efficient means to reduce the system installation costs. However, to demonstrate that the proposed strategy works properly in systems that are clustered in different sizes, the original scenarios were modified by varying the segmentation of 300 CUs. In addition to the original  $6 \times 50$  setup (6 clusters with 50 CUs per cluster), the cases with  $12 \times 25$  and  $20 \times 15$  were tested. In these tests, maximum reasonable under-sizing levels achieved via optimal LM were considered. The simulation results show that optimal LM achieves nearly identical results, that is, less than 0.5% deviation in energy supply in all scenarios.

### 7.3 | Long-term profits

The findings presented in Section 7.2 demonstrate that the optimal LM outperforms the benchmark LM in terms of the under-sizing level that it enables. To demonstrate overall economic impact of optimal LM, a high level economic analysis was conducted based on the metric,  $\pi$ , introduced in Section 4.3.

The parameters that were considered for cost and revenue calculations are shown in Table 8. The unit costs of the hardware components were obtained through normalisation of the parameters provided by a previous study [12] that estimates the hardware costs of a charging station with 300 EV chargers. In this analysis, an annual interest rate of 5% ( $r = 5\%$ ) was considered. The European wholesale market prices that occurred on 6 January 2020 [43] were used for the calculation of charging costs in each scenario. The revenues were calculated by multiplying the amount of energy supply with the flat tariff of 0.15 €/kWh.

Assuming that the scenarios will be repeated 300 times annually over the course of  $Y$  years, the long term net profits of the system were estimated by scaling the daily revenues and electricity bills of the charging station with  $300 \times Y$ . Table 9 provides the estimated net profits of 5 CPLs that exhibit one of the introduced scenarios repeatedly over 10 years. The table shows the estimated profits for benchmark and optimal LM under three sizing cases: exact sizing (0% under-sizing), benchmark sizing (maximum under-sizing via benchmark LM) and optimal sizing (maximum under-sizing via optimal LM).

The results reveal that under-sizing is an effective approach to increase the long term profits. For example, the 10-year net profit can be boosted by 22% in Scenario30 when the system is under-sized by 40%. Under benchmark sizing, optimal LM increases the long term profits slightly. A further reduction in the system down to the optimal sizing adds 3%–38% to long term profits as compared to benchmark sizing in the tested scenarios. However, when the benchmark LM is implemented at the optimal sizing level, such profit increases are achieved only by violating the condition (26). In this case, 10%–26% of

**TABLE 8** Cost/revenue parameters [12, 43–45]

| Cost component                       | Unit cost                       |
|--------------------------------------|---------------------------------|
| Transformer                          | 9000 Eur/MW                     |
| Power delivery elements of a cluster | 15,000 Eur/MW                   |
| EV chargers                          | 1000 Eur/11 kW                  |
| Grid fee ( $\kappa^g$ )              | 10,000 Eur/MW/year              |
| Electricity price in spot market     | $\kappa^e \in [33, 48]$ Eur/MWh |

**TABLE 9** 10-Year net profits in Euros

|            | Sizing    | U   | Benchmark LM | Optimal LM |
|------------|-----------|-----|--------------|------------|
| Scenario30 | Exact     | 0%  | 1 593 746    | 1 625 941  |
|            | Benchmark | 40% | 1 940 760    | 1 941 124  |
|            | Optimal   | 65% | 2 006 951    | 2 170 632  |
| Scenario40 | Exact     | 0%  | 1 652 092    | 1 694 215  |
|            | Benchmark | 30% | 1 912 334    | 1 914 190  |
|            | Optimal   | 60% | 2 046 436    | 2 191 493  |
| Scenario50 | Exact     | 0%  | 1 728 236    | 1 780 846  |
|            | Benchmark | 20% | 1 901 743    | 1 902 541  |
|            | Optimal   | 60% | 2 101 635    | 2 272 002  |
| Scenario60 | Exact     | 0%  | 1 808 486    | 1 871 687  |
|            | Benchmark | 10% | 1 895 151    | 1 899 127  |
|            | Optimal   | 60% | 2 165 094    | 2 356 551  |
| Scenario70 | Exact     | 0%  | 1 332 219    | 1 405 233  |
|            | Benchmark | 5%  | 1 375 175    | 1 384 173  |
|            | Optimal   | 70% | 1 899 805    | 1 970 883  |

the EVs in the tested scenarios leave the charging station with more than 1% unfulfilled demand.

To accurately quantify the improvement that optimal LM enables, one must compare the profits estimated for the benchmark LM under benchmark sizing with the results of optimal LM under optimal sizing since these are the maximum profits that can be achieved while meeting the satisfactory demand fulfilment rates. The comparison shows that the optimal LM in Scenario30 gives 12% rise to the 10-year profits. In Scenario70, the profits increase by 43% thanks to optimal LM. In other three scenarios, the additional profits acquired by optimal LM are between 15% and 25%.

To conclude the results of the economic analysis, the optimal LM makes it possible to achieve high demand fulfilment rates in heavily under-sized systems. The impact of optimal LM are particularly remarkable in the scenarios that include more long-time events. In the scenarios where more EVs have no or limited tolerance to supply interruptions, the increase in profits are less pronounced but still significant.

## 8 | SCALABILITY ANALYSIS

This section investigates the computational effort that is required to apply the proposed strategy in randomly generated scenarios to demonstrate its scalability and practicability. For this analysis, we solved the optimisation problems by the CPLEX [42] solver in a personal computer with an Intel(R) Core(TM) i5-8250U CPU @1.80 GH. The optimal scheduling and allocation steps of the proposed strategy are implemented sequentially upon EV arrivals. Therefore, the required time to execute scheduling plus allocation decisions determines the duration for an incoming EV to wait before the system operator sends it to a particular cluster in the system. To quantify the scalability of scheduling-allocation steps, we define 10 s as the maximum acceptable waiting time.

In repeated simulations, we tested several levels of temporal granularity, that is, horizon (estimated parking duration) and time resolution (size of time step,  $\Delta t$ ) of the optimisation problem. We varied the optimisation horizon as 4, 8, and 24 h and the resolution as 5 and 1 min. Furthermore, we solved optimal allocation problems with 16, 32, 64 and 128 clusters. Table 10 presents the mean computation times for each simulated case. The proposed strategy is able to find the

optimal solution for the joint scheduling-allocation problem that includes 16 cluster options and 1440 time steps (1-min resolution in 24 h) in much less than 10 s while, in case of 64 options for cluster selection, it can only deal with 288 time steps, which accounts for 5-min resolution in 24 h. When there are 128 candidate clusters in the system, no more than 48 time steps can be considered in the optimisation problem.

Table 10 depicts a linear increase in the computation time due to the increased number of time steps (left to right in the table). On the other hand, the impact of the number of clusters is exponential (top to bottom). This highlights that the number of integer variables, which is the number of clusters in the allocation problem, is more decisive for the overall computation time, and thereby for the scalability of the pre-connection steps of the proposed strategy.

The intervention step of the proposed strategy determines the real-time power references of the CUs; therefore, the time required to calculate the optimal values (computation time) must be sufficiently shorter than the duration for which the calculated references will be implemented (implementation time). We considered 5 min as both implementation time and the resolution of the optimisation problem. In repeated simulations, we increased the number of CUs gradually and calculated the mean computation time for the optimal intervention problem. The simulation results show that the optimal intervention model is able to find optimal references for up to 1760, 690 and 120 CUs in less than 5 s if, respectively, 6, 12 and 96 steps are considered in the optimisation problem.

It is important to note that the presented scalability metrics are dependent upon the hardware and software that the proposed strategy is applied with. In practical applications, it can be expected that an EV charging station comprising several hundreds of CUs could dedicate larger computational resource than what is used in this work. Nevertheless, the presented analyses show that the proposed strategy is practically applicable in scenarios with several hundreds of CUs despite a moderate computational capability.

## 9 | CONCLUSION

This study addresses the operational difficulty of large EV charging stations organised as under-sized charger clusters (UCC). Unless controlled, the load can concentrate into particular cluster(s) due to the heterogeneity of the behaviour of EVs. Uneven distribution of loads across the UCCs can lead to preventable supply interruptions. A load management strategy (LM) is introduced in this study to address this challenge. The LM strategy combines three optimisation models that, respectively, optimise the charging schedules (optimal scheduling), distribution of the vehicles among the charger clusters (optimal allocation) and short-term power references of charging units (optimal intervention). The optimal scheduling and allocation steps minimise the charging cost and inter-cluster unbalances, respectively. The operational boundaries of the power infrastructure are addressed in

**TABLE 10** Mean computation times for calculating optimal scheduling and allocation problems with various numbers of time steps and number of clusters

| Number of clusters | Number of time steps |       |       |       |        |        |
|--------------------|----------------------|-------|-------|-------|--------|--------|
|                    | 48                   | 96    | 240   | 288   | 960    | 1440   |
| 16                 | 0.21                 | 0.45  | 0.83  | 1.09  | 1.71   | 4.79   |
| 32                 | 0.50                 | 1.05  | 2.38  | 2.79  | 4.55   | 12.37  |
| 64                 | 1.90                 | 3.42  | 8.50  | 9.99  | 16.89  | 48.63  |
| 128                | 9.78                 | 20.19 | 49.66 | 67.01 | 116.68 | 312.90 |

the optimal intervention model. Without loss of generality, only the peak power limits of the clusters are considered in this study. Depending on specific application requirements, constraints beneath the peak power limits can be integrated into the management strategy by modifying only the intervention step.

The proposed strategy is tested in five commercial parking lot scenarios with various distribution of long and short time events and different tolerances for supply interruptions. Each step of the optimal management strategy is evaluated against a corresponding benchmark strategy: benchmark versus optimal scheduling, benchmark versus optimal allocation and benchmark versus optimal intervention. The results highlight the superiority of optimal strategies over benchmark strategies on the metrics of unit cost of charging and system energy supply. In addition to the comparison of individual steps of the benchmark versus optimal management, the whole of three-step optimal management is evaluated against the three-step benchmark management. It is demonstrated that the optimal strategy effectively increases the energy supply of the system with respect to the amount provided by the benchmark strategy in identically constrained scenarios. Such supply increase enables larger levels of under-sizing without decreasing the demand fulfilment prospects of the system.

As result of a high-level economic analysis, it is concluded that optimal management can boost the net 10-year profits of the charging station by more than 40% in certain scenarios. Furthermore, the scalability of the optimal strategy is investigated by analysing the computation times in scenarios at various scales. The results demonstrate that the strategy is practically applicable in scenarios with several hundreds of charging units even with a moderate computational capability of a personal computer. Future research should be devoted to the development of management concepts with consideration of bidirectional energy flow and investigation of vehicle-to-cluster, cluster-to-cluster and/or cluster-to-grid modes of operation in charging stations with UCC-based configurations.

## ACKNOWLEDGEMENTS

Modular Megawatt-range Wireless EV Charging Infrastructure Providing Smart Grid Services (MoMeWeC) is a research project (Grant number: 01DR18004) of the International Joint Initiative EIG CONCERT, Japan, under the Joint Call on Efficient Energy Storage and Distribution. The authors would like to thank German Federal Ministry of Education and Research (BMBF) and the Research Council of Norway for providing financial support.

Open access funding enabled and organized by Projekt DEAL.

## DATA AVAILABILITY STATEMENT

The data that support the findings of this study are available from the corresponding author upon reasonable request.

## ORCID

Erdem Gümrükcü  <https://orcid.org/0000-0002-6326-1668>

## REFERENCES

1. Abdulaal, A., et al.: Solving the multivariate ev routing problem incorporating V2G and G2V options. *IEEE Trans. Transp. Electr.* 3(1), 238–248 (2017)
2. Tu, H., et al.: Extreme fast charging of electric vehicles: a technology overview. *IEEE Trans. Transp. Electr.* 5(4), 861–878 (2019)
3. Choi, S.Y., et al.: Advances in wireless power transfer systems for roadway-powered electric vehicles. *IEEE J. Emerg. Select. Topics Power Electron.* 3(1), 18–36 (2015)
4. Clement-Nyns, K., Haesen, E., Driesen, J.: The impact of charging plug-in hybrid electric vehicles on a residential distribution grid. *IEEE Trans. Power Syst.* 25(1), 371–380 (2010)
5. Calearo, L., et al.: Grid loading due to EV charging profiles based on pseudo-real driving pattern and user behavior. *IEEE Trans. Transp. Electr.* 5(3), 683–694 (2019)
6. Leemput, N., et al.: Impact of electric vehicle on-board single-phase charging strategies on a Flemish residential grid. *IEEE Trans. Smart Grid.* 5(4), 1815–1822 (2014)
7. Lopes, J.A.P., Soares, F.J., Almeida, P.M.R.: Integration of electric vehicles in the electric power system. *Proc. IEEE.* 99(1), 168–183 (2011)
8. ElNozahy, M.S., Salama, M.M.A.: A comprehensive study of the impacts of PHEVs on Residential Distribution Networks. *IEEE Trans. Sustain. Energy.* 5(1), 332–342 (2014)
9. Brenna, M., et al.: Charging optimization for electric vehicles in large park and ride areas. In: 2016 IEEE Power and Energy Society General Meeting (PESGM), pp. 1–5. (2016)
10. Su, W., Chow, M.: Performance evaluation of an EDA-based large-scale plug-in hybrid electric vehicle charging algorithm. *IEEE Trans. Smart Grid.* 3(1), 308–315 (2012)
11. Recalde Melo, D.F., Hoay Beng, G., Massier, T.: Charging of electric vehicles and demand response management in a Singaporean Car Park. In: 2014 49th International Universities Power Engineering Conference (UPEC), pp. 1–6. (2014)
12. Strickland, D., et al.: Feasibility study: investigation of car park-based V2G services in the UK Central Hub. *J. Eng.* 2019(17), 3967–3971 (2019)
13. Guidi, G., et al.: Load balancing of a modular multilevel grid-interface converter for transformer-less large-scale wireless electric vehicle charging infrastructure. *IEEE J. Emerg. Select. Topics Power Electron.* 9(4), 4587–4605 (2021)
14. Liu, Z., et al.: Optimal planning of charging station for electric vehicle based on particle swarm optimization. In: *IEEE PES Innovative Smart Grid Technologies*, pp. 1–5. (2012)
15. Hussain, A., Bui, V., Kim, H.: Optimal sizing of battery energy storage system in a fast EV charging station considering power outages. *IEEE Trans. Transp. Electr.* 6(2), 453–463 (2020)
16. Yao, L., Lim, W.H., Tsai, T.S.: A real-time charging scheme for demand response in electric vehicle parking station. *IEEE Trans. Smart Grid.* 8(1), 52–62 (2017)
17. Chandra Mouli, G.R., et al.: Integrated PV charging of EV fleet based on energy prices, V2G, and offer of reserves. *IEEE Trans. Smart Grid.* 10(2), 1313–1325 (2019)
18. Rabiee, A., Ghiasian, A., Chermahini, M.A.: Long term profit maximization strategy for charging scheduling of electric vehicle charging station. *IET Gener. Transm. Distrib.* 12, 4134–4141 (2018)
19. Mukherjee, J.C., Gupta, A.: A review of charge scheduling of electric vehicles in smart grid. *IEEE Syst. J.* 9(4), 1541–1553 (2015)
20. Nimalsiri, N.I., et al.: A survey of algorithms for distributed charging control of electric vehicles in smart grid. *IEEE Trans. Intell. Transp. Syst.* 21(11), 4497–4515 (2020)
21. Abdullah, H.M., Gastli, A., Ben-Brahim, L.: Reinforcement learning based EV charging management systems – a review. *IEEE Access.* 9, 41506–41531 (2021)
22. Yin, H., Alsabbagh, A., Ma, C.: A decentralized power dispatch strategy in an electric vehicle charging station. *IET Electr. Syst. Transp.* 11(1), 25–35 (2021)

23. Wang, D., et al.: Integrated energy exchange scheduling for multi-microgrid system with electric vehicles. *IEEE Trans. Smart Grid.* 7(4), 1762–1774 (2016)
24. Shi, Y., et al.: Model predictive control for smart grids with multiple electric-vehicle charging stations. *IEEE Trans. Smart Grid.* 10(2), 2127–2136 (2019)
25. Li, Y., et al.: Coordinating flexible demand response and renewable uncertainties for scheduling of community integrated energy systems with an electric vehicle charging station: a bi-level approach. *IEEE Trans. Sustain. Energy.* 1 (2021)
26. Kuran, M.S., et al.: A smart parking lot management system for scheduling the recharging of electric vehicles. *IEEE Trans. Smart Grid.* 6(6), 2942–2953 (2015)
27. Shahriar, S., et al.: Machine learning approaches for EV charging behavior: a review. *IEEE Access.* 8, 168980–168993 (2020)
28. Ashkrof, P., Homem de Almeida Correia, G., van Arem, B.: Analysis of the effect of charging needs on battery electric vehicle drivers' route choice behaviour: a case study in The Netherlands. *Transp. Res. Transp. Environ.* 78, 102206 (2020)
29. Tomaszewska, A., et al.: Lithium-ion battery fast charging: a review. *eTransportation.* 1, 100011 (2019)
30. Rivera, S., et al.: Electric vehicle charging station using a neutral point clamped converter with bipolar DC bus. *IEEE Trans. Ind. Electron.* 62(4), 1999–2009 (2015)
31. Bai, S., Lukic, S.M.: Unified active filter and energy storage system for an MW electric vehicle charging station. *IEEE Trans Power Electron.* 28(12), 5793–5803 (2013)
32. Tabari, M., Yazdani, A.: An energy management strategy for a DC distribution system for power system integration of plug-in electric vehicles. *IEEE Trans. Smart Grid.* 7(2), 659–668 (2016)
33. Moghaddam, Z., et al.: Smart charging strategy for electric vehicle charging stations. *IEEE Trans. Transp. Electrification.* 4(1), 76–88 (2018)
34. Hu, J., et al.: Coordinated charging of electric vehicles for congestion prevention in the distribution grid. *IEEE Trans. Smart Grid.* 5(2), 703–711 (2014)
35. Hu, J., et al.: Preventing distribution grid congestion by integrating indirect control in a hierarchical electric vehicles' management system. *IEEE Trans. Transp. Electrification.* 2(3), 290–299 (2016)
36. Liu, J., et al.: Optimal logistics EV charging scheduling by considering the limited number of chargers. *IEEE Trans. Trans. Electrification.* 1 (2020)
37. Gümrükcü, E., et al.: V2G potential estimation and optimal discharge scheduling for MMC-based charging stations. In: 2020 5th IEEE Workshop on the Electronic Grid (eGRID), pp. 1–6. (2020)
38. Gümrükcü, E., et al.: Optimized allocation of loads in MMC-based electric vehicle charging infrastructure. In: 2020 IEEE International Conference on Power Systems Technology (POWERCON), pp. 1–6. (2020)
39. He, Y., Venkatesh, B., Guan, L.: Optimal scheduling for charging and discharging of electric vehicles. *IEEE Trans. Smart Grid.* 3(3), 1095–1105 (2012)
40. Smart Grid Traffic Light Concept. BDEW –German Association of Energy and Water Industries (2015)
41. Hart, W.E., et al.: *Pyomo—Optimization Modeling in Python*, vol. 67, 2nd ed. Springer Science & Business Media (2017)
42. CPLEX. Accessed 2020-04-01. <https://www.ibm.com/de-de/products/ilog-cplex-optimization-studio>
43. European Electricity Index (ELIX). Accessed: 2020-03-31. <https://www.epexspot.com/en>
44. Stadtwerke Aachen AG (STAWAG). Accessed: 2020-03-31. <https://www.stawag.de>
45. Regulatory Framework for RES-E System Integration in Europe – Description and Analysis of Different European Practices. GreenNet-Incentives, Standard (2009)

**How to cite this article:** Gümrükcü, E., et al.: Optimal load management strategy for large electric vehicle charging stations with undersized charger clusters. *IET Electr. Syst. Transp.* 1–16 (2021). <https://doi.org/10.1049/els2.12037>